EVLA Off–axis Beam and Instrumental Polarization

W. D. Cotton and R. Perley, January 7, 2010

Abstract—This memo describes measurements of the polarization properties of the EVLA antennas at a variety of frequencies. The antennas will introduce weak off-axis linear polarization and, due to the beam squint, a strong off–axis circular instrumental polarization. Well off–axis, the beam power response shows strong azimuthal asymmetries. A technique of correcting for antenna beam assymmetries and removing off–axis instrumental polarization using the beam polarization images and a total intensity model of the emission in the beam is described. The EVLA beam responses are very close to being real functions. The measured L band polarization is similar to, but different in detail, from electromagnetic calculations of the VLA beam.

Index Terms—interferometry, calibration, polarimetry

I. INTRODUCTION

ANY given photon has a well defined polarization state but the aggregate signal from an incoherent astronomical source will have photons with a distribution of polarization states. The polarization of such a signal is described by statistical measures giving the relative numbers of photons in a set of orthogonal states; zero polarization is equal numbers in the orthogonal states and 100% is all photons in one state. The principle components of polarization are circular, where the E–vectors trace circles as they propagate in either a right– or left–handed fashion; or where the E–vectors are confined to a line (linear polarization) and the orthogonal states are orthogonal orientations of the lines of polarization. In practice, a given signal will be a combination of these two, or elliptically polarized. The polarization of an astronomical signal tells a great deal about the emission process (e.g. thermal sources are unpolarized, synchrotron highly linearly polarized) as well as the transmission of the signals through the intervening media (e.g. Faraday rotation of linearly polarized signals).

Reflections of radio signals will generally affect the polarization state of the outgoing signal; this may change the statistics of the various polarization states possibly leading to the spurious polarization of the signal. Accurate, polarimetry requires the estimation and removal of any spurious instrumental polarized response to an unpolarized signal.

Radio astronomical antennas are designed such that the polarizations introduced in the signal in various portions of the antenna are balanced, resulting in a net cancellation and no net instrumental linear polarization. This can be only strictly true at one position in the beam, usually the on–axis location. Polarization is generally described in terms of the Stokes parameters I (total intensity), Q and U (linear polarization) and V (circular polarization).

W. D. Cotton, National Radio Astronomy Observatory, 520 Edgemont Rd., Charlottesville, VA, 22903 USA email: bcotton@nrao.edu

R. Perley, National Radio Astronomy Observatory, 1003 Lopezville Rd., Socorro, NM, 87801 USA email: rperley@nrao.edu

Wide field images even in Stokes I will be affected by any azimuthal asymmetries in the antenna power patterns. Such asymmetries will be created by mechanical structures in the incoming beam such as subreflector support legs. These asymmetries can introduce imaging artifacts that limit the dynamic range of the image.

This memo explores the off–axis component of the gain and instrumental polarization of the EVLA antennas and a technique to correct visibility measures. The technique described here has been implemented in the calibration and imaging software in the Obit package [1] [1].

II. INSTRUMENTAL POLARIZATION

Spurious instrumental polarization can come from a variety of different causes and may generally be divided into an on–axis and an off–axis component. Measurements of, and corrections for, on–axis instrumental polarization have long been standard practice[2]. Off–axis linear polarization is usually weak in the inner portion of the beam and tends to average out for long integrations. Off–axis instrumental polarization corrections were made to the snapshot images of the NVSS [3] survey [4].

Antennas of the design of the (E)VLA, VLBA and ALMA antennas have a special problem with circular polarization. The off-axis mounting of the feeds introduces a "beam squint" which causes the orthogonally polarized beams to be offset on the sky [5][6]. For the (E)VLA and VLBA, this introduces a strong off–axis circular polarization which has severely limited the use of these instruments for measuring circular polarization. An off–axis correction technique for circular polarization based on a model beam-shape and estimates of the squint offset of the RCP and LCP beams on the sky is described in [7]. Such corrections can also be made on the basis of the measured response of the telescope. Modeling of the EVLA antenna response is described in [8].

III. GAIN AND POLARIZATION MEASUREMENTS

Beam gain and polarization measurements were made on EVLA antennas using the VLA correlator in holography mode in which the beam was mapped using rasters in azimuth and elevation. The array was in D configuration. The beam was mapped at "low" resolution using a 17×17 raster spaced by $0.25 * \lambda/D$ where λ is the reference wavelength and D is the antenna diameter in meters. At selected frequencies, the beam was also mapped at higher resolution over a smaller portion of the beam. At each pointing, 3×1.67 second samples were recorded.

[1]http://www.cv.nrao.edu/∼bcotton/Obit.html

The holography mode observations were calibrated in the standard methods in AIPS[2] and then imaged in Obit task MapBeam. MapBeam applies the standard calibrations and averages the data over selected baselines in each IF/Stokes correlation and pointing. Pointing offsets in azimuth and elevation from the source position are given in the visibility "u" and "v" coordinates in radians (see section III-A). The average pointing value for Q, U and V correlations were normalized by that for Stokes I. The linear polarization, Q+jU, was counter–rotated by the parallactic angle applied in calibration:

$$Q' + jU' = (Q + jU) * exp(-2j\chi)$$

where Q and U are the measured, averaged and normalized Stokes Q and U correlations, Q' and U' are the rotated values and χ, the parallactic angle, is given by:

$$\chi = atan2\{cos(Lat)sin(HA),$$
$$(sin(Lat)cos(\delta) - cos(Lat)sin(\delta)cos(HA))\},$$

where Lat is the latitude of the antenna, HA is the hour angle of the observation and δ the declination of the source.

The actual grid of measurements was almost, but not exactly, on the desired grid, so a Lagrangian interpolation using the nearest 3×3 cells was used to determine the final griding of the data. The calibrator observed may have an intrinsic polarization which will remain even after on–axis instrumental polarization calibration. To correct for this, the value in the on–axis pixel of the Q and U images was multiplied by the Stokes I beam images and subtracted from the Q and U images. Finally, the Stokes I image was normalized by the value in the on–axis pixel.

The beam images derived are complex although the imaginary parts are generally small. A set of "Real" images were made from the amplitude of the complex images with negative values where the phase is closer to $\pm180°$ than $0°$. Optionally, phase images can also be made.

There are two modes of deriving beam images, The first is a holographic mode in which one or more "reference antennas" remain pointed at the strong source while the remainder trace the beam raster. Such measurements map the voltage beams of the antennas. The second mode is one in which all antennas used are moved in the raster pattern; this measures the power pattern of the antennas. In the following, the measures of the antenna power pattern are considered.

A. VLA Holography Mode Data

Data from the VLA on-line system taken in the holography mode used to make beam maps has the pointing offset in the interferometric "u" and "v" coordinates. The u coordinate is the offset of the antenna from the source position in azimuth (from N thru E) in radians and "v" is the offset of the source from the antenna pointing in radians. The position of the source in the beam is (azimuth,elevation) = (-u,v).

B. L Band

1) Low Resolution: L band measurements were made in 2×50 MHz bands at 1.4649 and 1.3851 GHz on the weakly linearly polarized calibrator 0542+498 (3C147). The measurements consisted of a 17×17 raster with a spacing of 429.5". The flux density calibrators used were 0542+498 for which flux densities of 21.45 and 22.35 Jy were assumed for the two IFs, 0521+166 (3C138) for which flux densities of 8.17 and 8.44 Jy were assumed, and 1331+305 (3C286) for which flux densities of 14.51 and 14.90 were assumed. The astrometric (and Stokes V) calibrator was 0542+498. The on–axis instrumental polarization calibrators were 0521+166, 0542+498 and 1331+305. The beam images are shown in Figure 1. The reference antenna was number 7.

2) High Resolution: Higher resolution L band measurements were made in 2×50 MHz bands at 1.465 and 1.865 GHz on the weakly linearly polarized calibrator 0542+498 . The measurements consisted of a 19×19 raster with a spacing of 245.4". A second set of rasters were attempted at 1.650 and 1.200 GHz but were rendered useless by strong interference. The flux density calibrators used were 0137+331 (3C48) with assumed flux densities of 15.49 and 12.74 were assumed for the two IFs and 0542+498 for which flux densities of 21.45 and 17.86 Jy were assumed for the two IFs. The astrometric (and Stokes V) calibrator was 0542+498. The polarization angle calibrator was 0137+331 and the assumed R-L phase was -33° at 1.4649 and 26° at 1.8649 GHz. The on–axis instrumental polarization calibrators were 0137+331 and 0542+498. The beam images are shown in Figure 2. The reference antennas were number 14 and 18.

C. S Band

1) Low Resolution: S band measurements were made in 2×50 MHz bands at 3.2851 and 3.7851 GHz on the weakly linearly polarized calibrator 0542+498. The measurements consisted of a 17×17 raster with a spacing of 189.7". The flux density calibrators used were 0542+498 for which flux densities of 11.23 and 9.93 Jy were assumed for the two IFs and 1331+305 for which flux densities of 9.47, 8.72 were assumed. The astrometric (and Stokes V) calibrator was 0542+498. The beam images are shown in Figure 3. The reference antenna was number 24. Beam images were made with 3 antennas, no linear polarization was available.

2) High Resolution: Higher resolution S band measurements were made in 2×50 MHz bands at 2.750 and 2.250 GHz on the weakly linearly polarized calibrator 0542+498. A second pair of 50 MHz were also used at 3.25 and 3.75 GHz. The measurements consisted of a 17×17 raster with a spacing of 189.7" for the first pair and 151.0" for the second pair of frequencies. Only four non–reference antennas were available. The flux density calibrators used were 0137+331 (3C48) with assumed flux densities of 9.14 Jy (2.750 GHz), 10.88 Jy (2.250 GHz), 7.88 Jy (3.25 GHz) and 6.92 Jy (3.75 GHz) and 0542+498 for which flux densities 13.06 Jy (2.750 GHz), 15.39 Jy (2.250 GHz), 11.34 Jy ((3.25 GHz) and 10.01 Jy (3.75 GHz) were assumed. The astrometric (and Stokes V) calibrator was 0542+498. The polarization angle calibrator
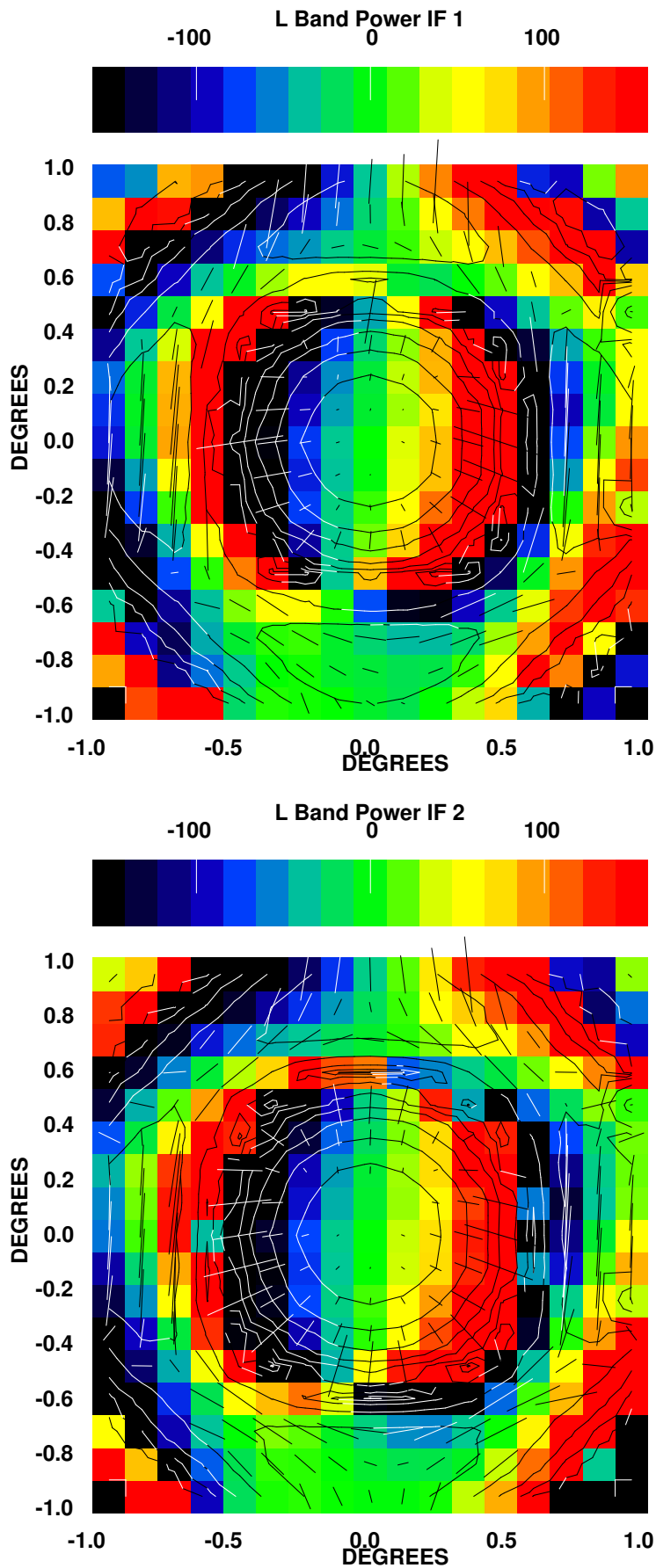
Fig. 1. L band power beam images in azimuth and elevation; IF 1 (1.4649 GHz) upper, IF 2 (1.3851 GHz) lower. Normalized total intensity is shown as contours in powers of 2 from 0.001, highest is 0.512. Stokes V is shown in color with the scale bar at the top in units of 0.001. Fractional linear polarization is represented by vectors, one pixel = 0.05.
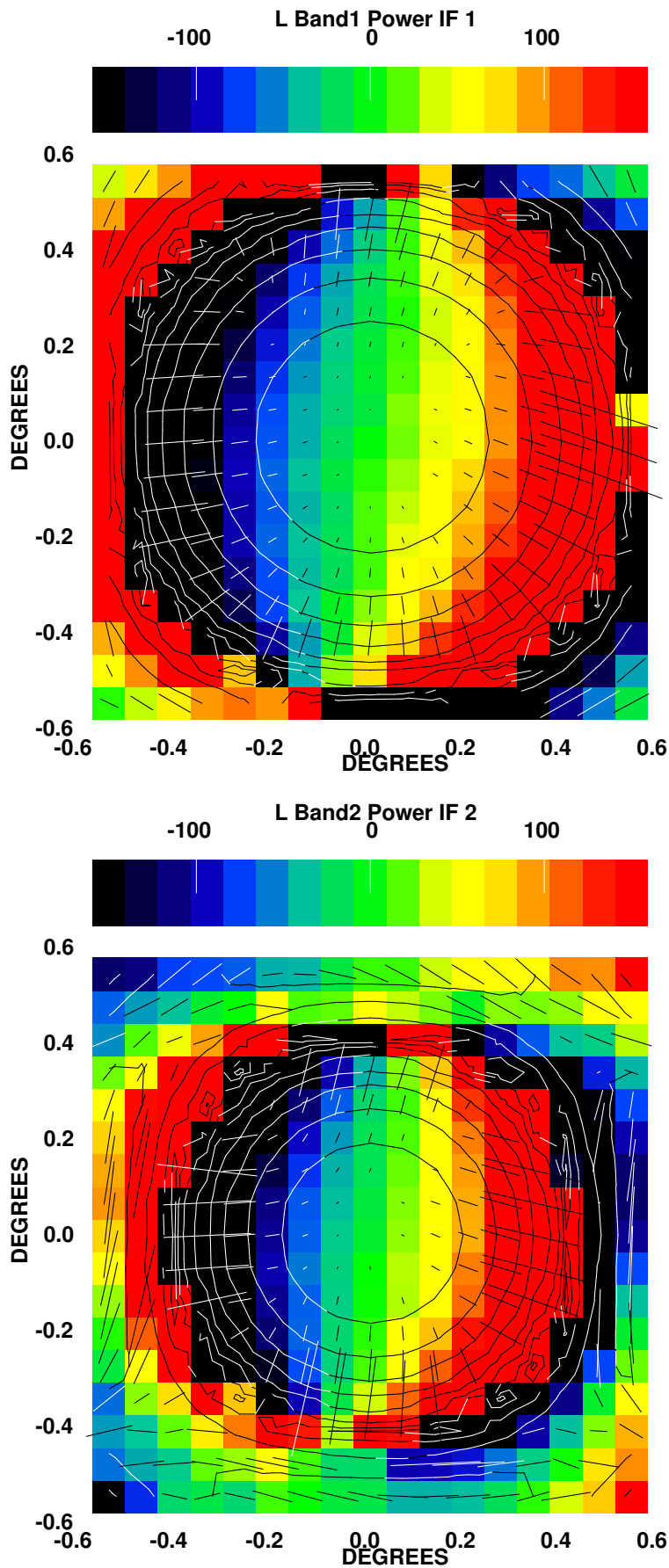
Fig. 2. High resolution L band power beam images in azimuth and elevation; IF 1 (1.4649 GHz) upper, IF 2 (1.8649 GHz) lower. Normalized total intensity is shown as contours in powers of 2 from 0.001, highest is 0.512. Stokes V is shown in color with the scale bar at the top in units of 0.001. Fractional linear polarization is represented by vectors, one pixel = 0.05.
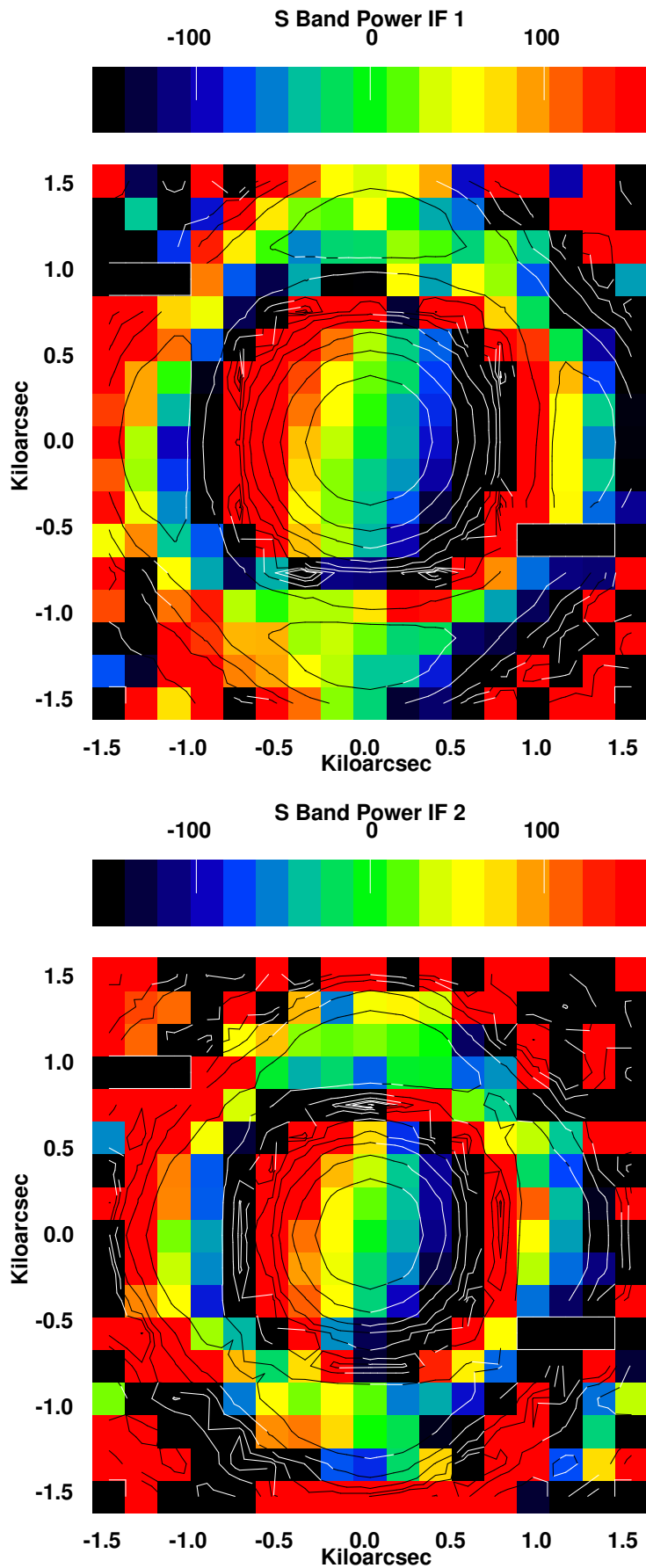
Fig. 3. S band power beam images in azimuth and elevation; IF 1 (3.2851 GHz) upper, IF 2 (3.7851 GHz) lower. Normalized total intensity is shown as contours in powers of 2 from 0.001, highest is 0.512. Stokes V is shown in color with the scale bar at the top in units of 0.001. Linear polarization was not measured.
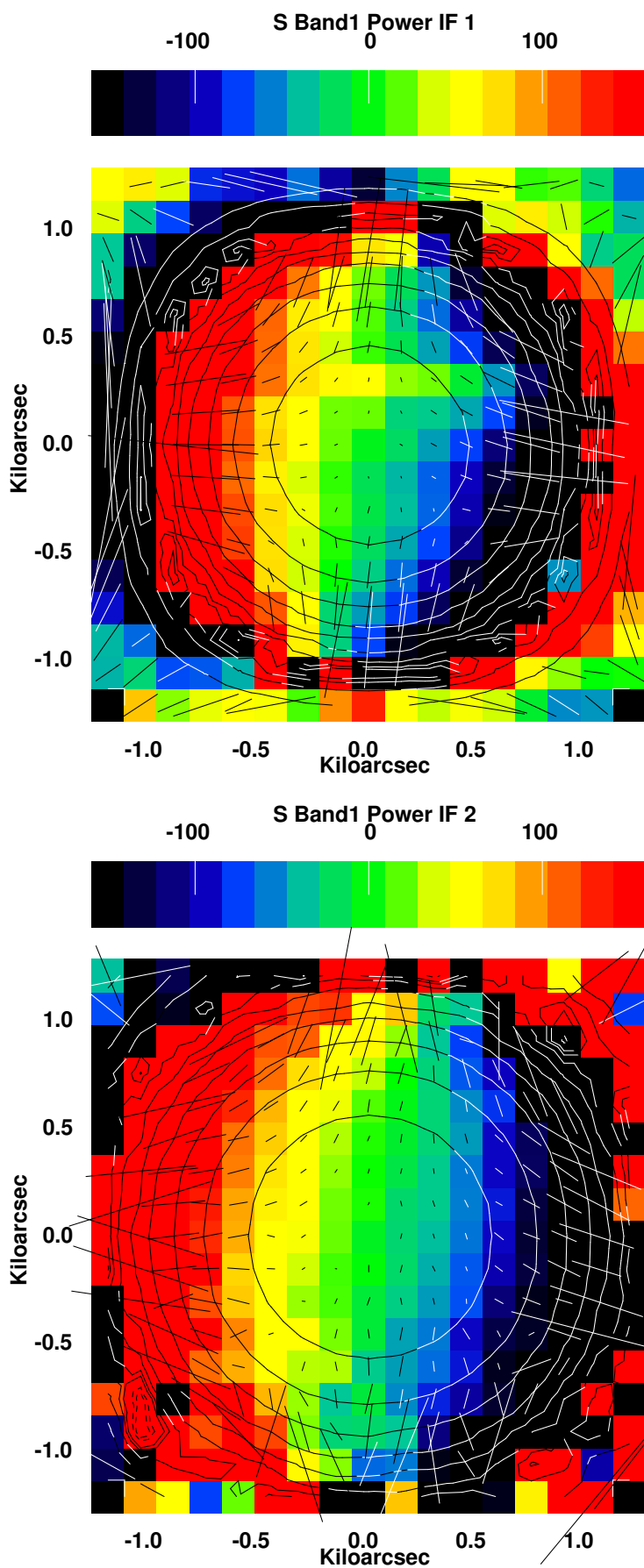
Fig. 4.   High resolution pair 1 S band power beam images in azimuth and elevation; IF 1 (2.750 GHz) upper, IF 2 (2.250 GHz) lower. Normalized total intensity is shown as contours in powers of 2 from 0.001, highest is 0.512. Stokes V is shown in color with the scale bar at the top in units of 0.001. Only four antennas were used. Fractional linear polarization is represented by vectors, one pixel = 0.05.

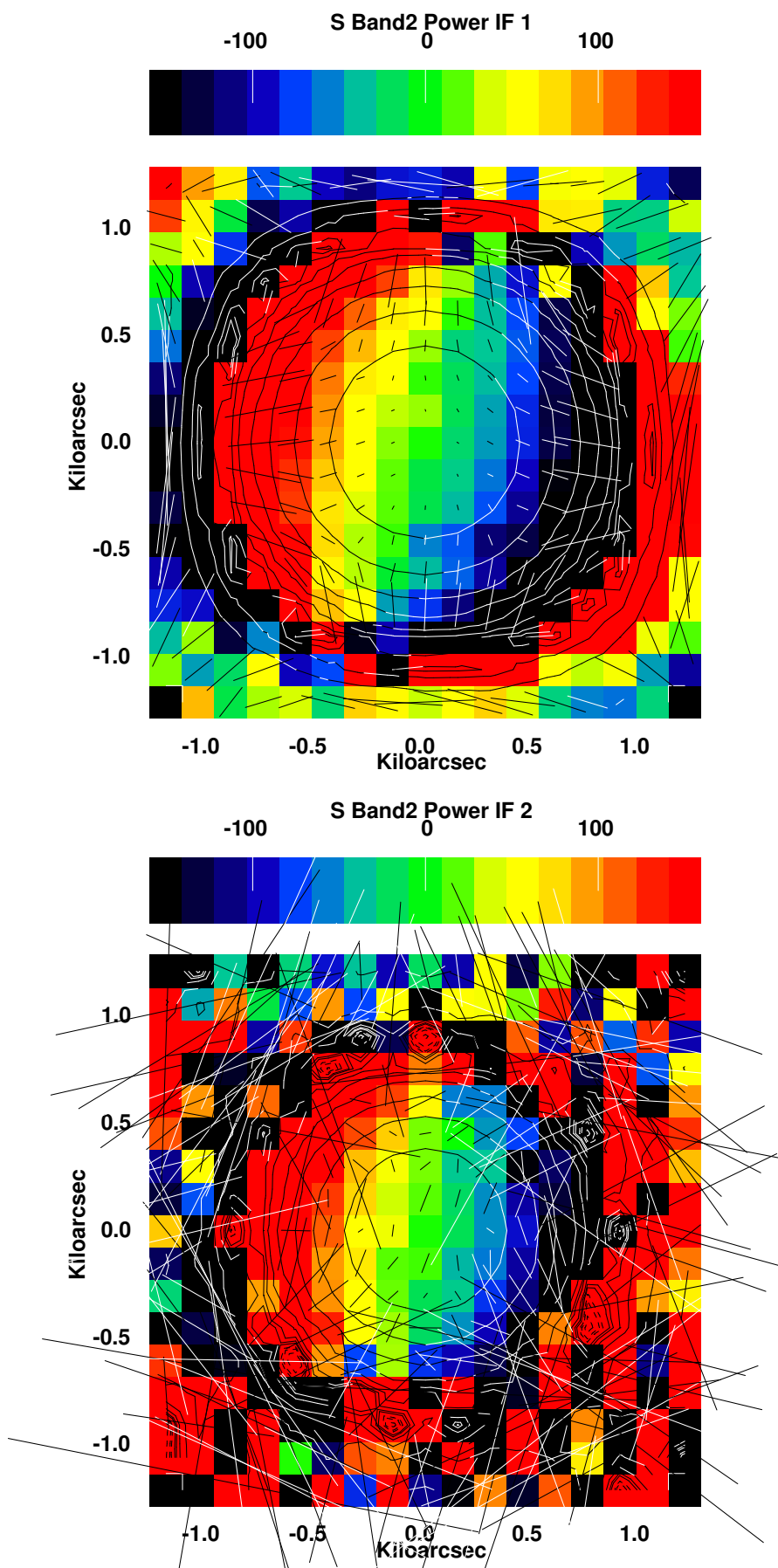**S Band2 Power IF 1**

S Band2 Power IF 2

Fig. 5. High resolution pair 2 S band power beam images in azimuth and elevation; IF 1 (3.250 GHz) upper, IF 2 (3.750 GHz) lower. Normalized total intensity is shown as contours in powers of 2 from 0.001, highest is 0.512. Stokes V is shown in color with the scale bar at the top in units of 0.001. Only four antennas were used. Fractional linear polarization is represented by vectors, one pixel = 0.05.

was 0137+331 and the assumed R-L phase was 96.5° at 3.750 GHz, 88.7° at 3.250 GHz, 76° at 2.750 GHz and 55° at 2.250 GHz. The on–axis instrumental polarization calibrators were 0137+331 and 0542+498. The beam images are shown in Figures 4 and 5. The reference antenna was number 24.

D. C Band

1) Low Resolution: C band measurements were made in 2×50 MHz bands at 4.8851 and 4.8351 GHz of the weakly linearly polarized calibrator 0319+415 (3C84). The measurements consisted of a 17×17 raster with a spacing of 127.2". The flux density calibrator used was 0137+331 for which flux densities of 5.40 and 5.46 Jy was assumed for the two IFs. The astrometric (and Stokes V) calibrator was 0319+415 (Note circularly polarized calibrator). The on–axis instrumental polarization calibrators were 0137+331 and 0319+415. The beam images are shown in Figure 6. The reference antenna was number 7.

2) High Resolution: Higher resolution C band measurements were made in 2×50 MHz bands at 4.50 and 6.50 GHz of the weakly linearly polarized calibrator 0542+498. A second pair of 50 MHz were also used at 5.50 and 7.50 GHz. The measurements consisted of a 17×17 raster with a spacing of 79.0" for the first pair and 92.0" for the second pair. The flux density calibrators used were 0137+331 (3C48) with assumed flux densities of 5.84 Jy (4.50 GHz), 4.1 Jy (6.50 GHz), 4.83 Jy (5.50 GHz) and 3.56 Jy (7.50 GHz) and 0542+498 for which flux densities 8.52 Jy (4.50 GHz), 6.08 Jy (6.50 GHz), 7.10 Jy (5.50 GHz) and 5.32 Jy (7.50 GHz) were assumed. The astrometric (and Stokes V) calibrator was 0542+498. The on–axis instrumental polarization calibrators were 0137+331 and 0542+498. The beam images are shown in Figures 7 and 8. The reference antenna was number 18.

E. X band

X band measurements were made in 2×50 MHz bands at 8.4351 and 8.4851 GHz on the weakly linearly polarized calibrator 0319+415. The measurements consisted of a 17×17 raster with a spacing of 73.1". The flux density calibrator used was 0137+331 for which flux densities of 3.16 and 3.15 Jy was assumed for the two IFs. The astrometric (and Stokes V) calibrator was 0319+415 (Note circularly polarized calibrator). The on–axis instrumental polarization calibrators were 0137+331 and 0319+415. The beam images are shown in Figure 9. The reference antenna was number 7.

F. K Band

K band measurements were made in 2×50 MHz bands at 22.485 and 22.435 GHz on the weakly linearly polarized calibrator 0319+415. The measurements consisted of a 17×17 raster with a spacing of 27.5". The flux density calibrator used was 0137+331 for which a flux density of 1.12 Jy was assumed for both IFs. The astrometric (and Stokes V) calibrator was 0319+415 (Note circularly polarized calibrator). The on–axis instrumental polarization calibrators were 0137+331 and 0319+415. The beam images are shown in Figure 10. The reference antenna was number 7.

G. Ka Band

Ka band measurements were made in 2×50 MHz bands at (33.485 and 33.435 GHz on the weakly linearly polarized calibrator 0319+415. The measurements consisted of a 17×17 raster with a spacing of 18.5". The flux density calibrators used were 0137+331 for which flux densities of 0.71 Jy was assumed for the two IFs and 0521+166 for which the assumed flux density was 0.71 Jy. The astrometric (and Stokes V) calibrator was 0319+415 (Note circularly polarized calibrator). The on–axis instrumental polarization calibrators were 0137+331, 0319+415 and 0521+166 The beam images are shown in Figure 11. The reference antenna was number 7.

H. Q Band

Q band measurements were made in 2×50 MHz bands at 43.315 and 43.365 GHz on the weakly linearly polarized calibrator 0319+415. The measurements consisted of a 17×17 raster with a spacing of 14.3". The flux density calibrators used were 0137+331 for which flux densities of 0.53 Jy was assumed for the two IFs and 0521+166 for which the assumed flux density was 0.54 Jy. The astrometric (and Stokes V) calibrator was 0319+415 (Note circularly polarized calibrator). The on–axis instrumental polarization calibrators were 0137+331, 0319+415, and 0521+166. The beam images are shown in Figure 12. The reference antenna was number 7.

IV. COMPARISON WITH MODEL

The beam images at L band can be compared with the electromagnetic modeling by Brisken[8]. The model calculation was performed for the VLA feed location rather than that of the EVLA antennas but the comparison is still instructive. Figure 13 compares Figure 3 of [8] with the comparable plot for the measured polarization beam at one L band frequency. The measured and model beams have basic similarities but differ in detail. The inner portion of the measured beam show somewhat larger fractional linear polarization and the polarization vectors are not strictly radial as they are in the model beam. The model polarization pattern is offset from the beam center whereas the measured beam is not.

V. OFF-AXIS BEAM CORRECTION

Deviations of the actual antenna beam response from an ideal response will introduce artifacts into wide field images derived from such antennas; knowledge of the actual antenna response can be used to correct the artifacts introduced. Such corrections are easily applied in a CLEAN deconvolution by using the knowledge of where in the antenna pattern a given CLEAN component is being observed at a given time. For alt–az mounted antenna this location will rotate with parallactic angle as the antenna track the celestial position. The following sections discuss corrections in total intensity and polarization.

A. Gain Correction

As can be readily seem in Figures 1 – 12, the beam pattern far from the pointing center is not azimuthially symmetric. During an extended synthesis, the gain in the directions of
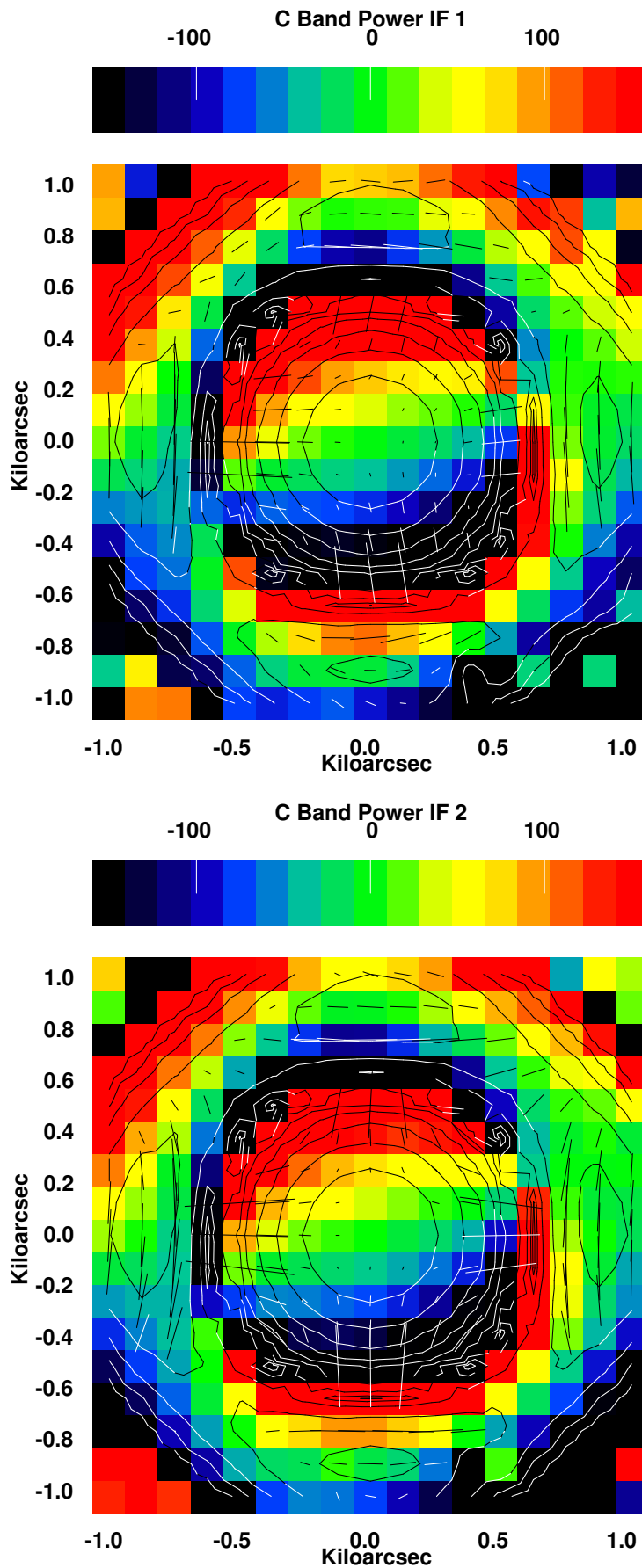
Fig. 6.   C band power beam images in azimuth and elevation; IF 1 (4.8851 GHz) upper, IF 2 (4.8351 GHz) lower. Normalized total intensity is shown as contours in powers of 2 from 0.001, highest is 0.512. Stokes V is shown in color with the scale bar at the top in units of 0.001. Fractional linear polarization is represented by vectors, one pixel = 0.05.
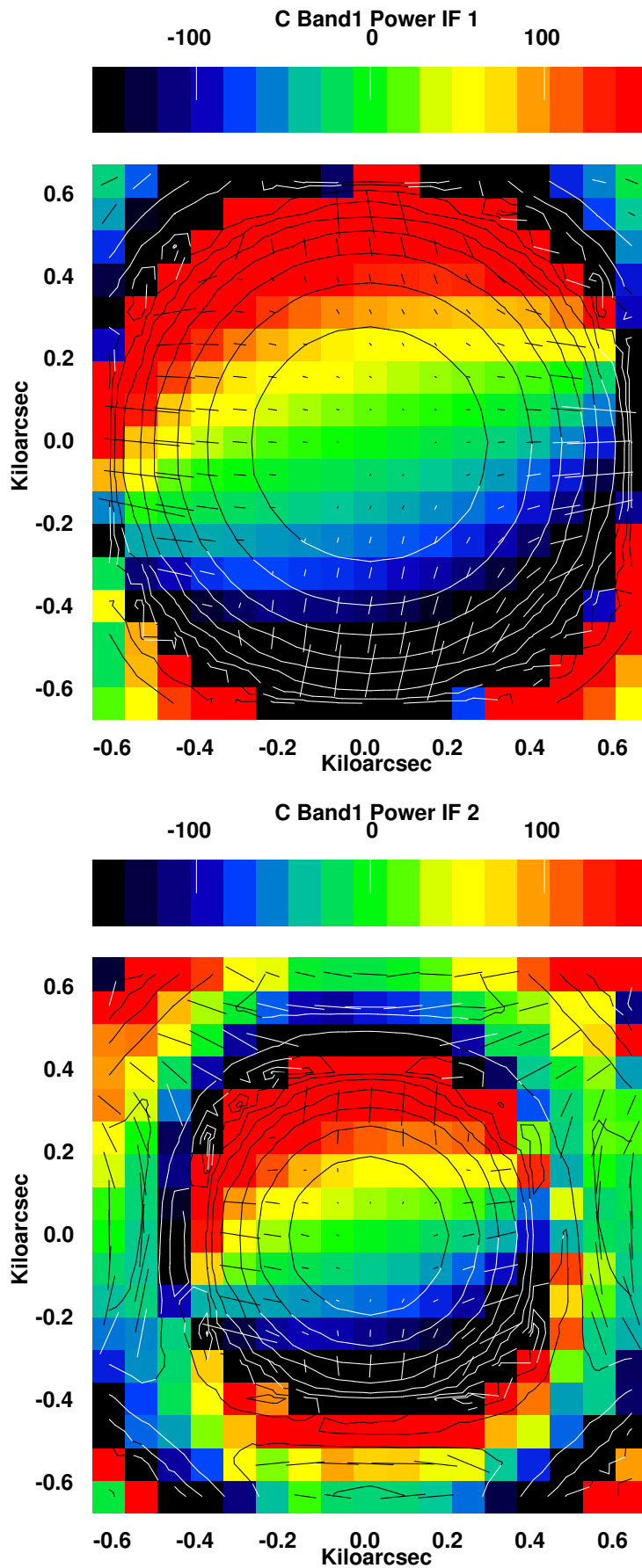
Fig. 7. High resolution pair 1 C band power beam images in azimuth and elevation; IF 1 (4.50 GHz) upper, IF 2 (6.50 GHz) lower. Normalized total intensity is shown as contours in powers of 2 from 0.001, highest is 0.512. Stokes V is shown in color with the scale bar at the top in units of 0.001. Fractional linear polarization is represented by vectors, one pixel = 0.05.
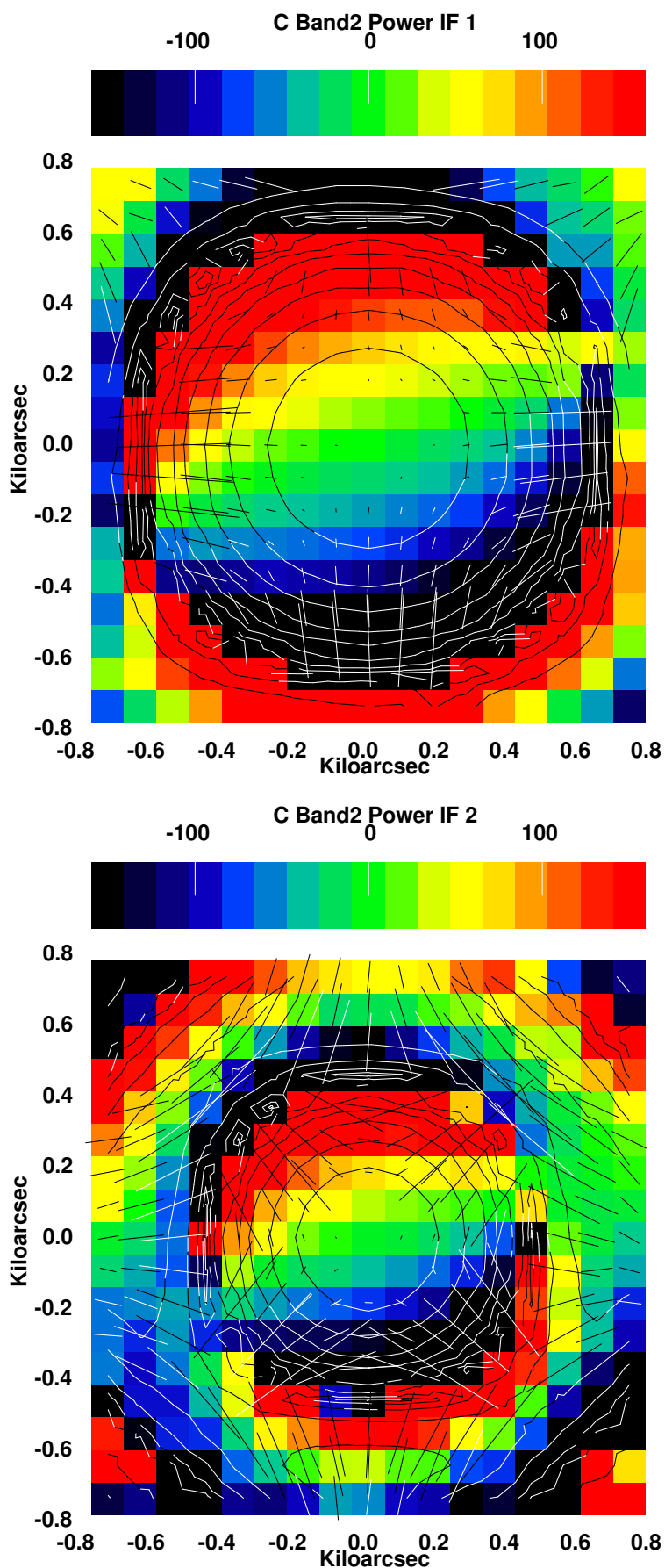
Fig. 8. High resolution pair 2 C band power beam images in azimuth and elevation; IF 1 (5.50 GHz) upper, IF 2 (7.50 GHz) lower. Normalized total intensity is shown as contours in powers of 2 from 0.001, highest is 0.512. Stokes V is shown in color with the scale bar at the top in units of 0.001. Fractional linear polarization is represented by vectors, one pixel = 0.05.
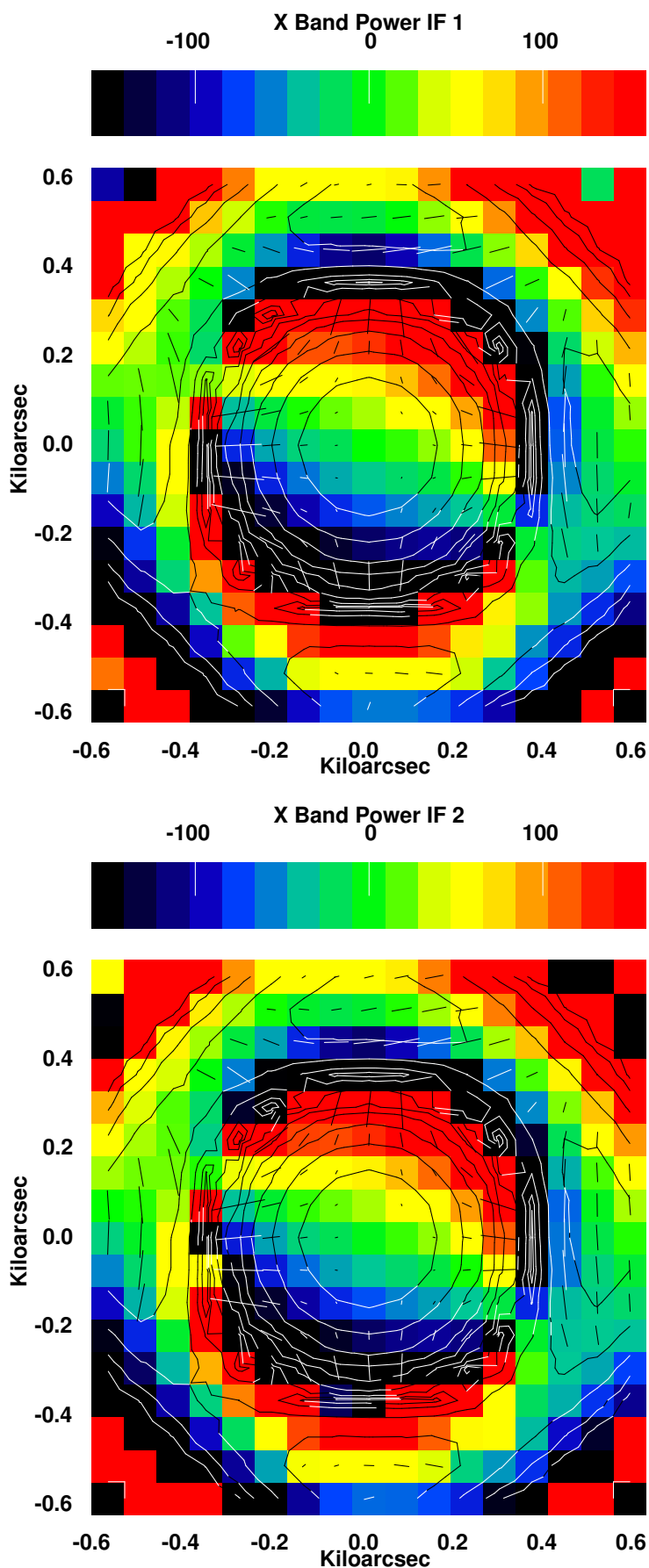
Fig. 9. X band Power beam images in azimuth and elevation; IF 1 (8.4351 GHz) upper, IF 2 (8.4851 GHz) lower. Normalized total intensity is shown as contours in powers of 2 from 0.001, highest is 0.512. Stokes V is shown in color with the scale bar at the top in units of 0.001. Fractional linear polarization is represented by vectors, one pixel = 0.05.

Fig. 10.   K band power beam images in azimuth and elevation; IF 1 (22.485 GHz) upper, IF 2 (22.435 GHz) lower. Normalized total intensity is shown as contours in powers of 2 from 0.001, highest is 0.512. Stokes V is shown in color with the scale bar at the top in units of 0.001. Fractional linear polarization is represented by vectors, one pixel = 0.05.
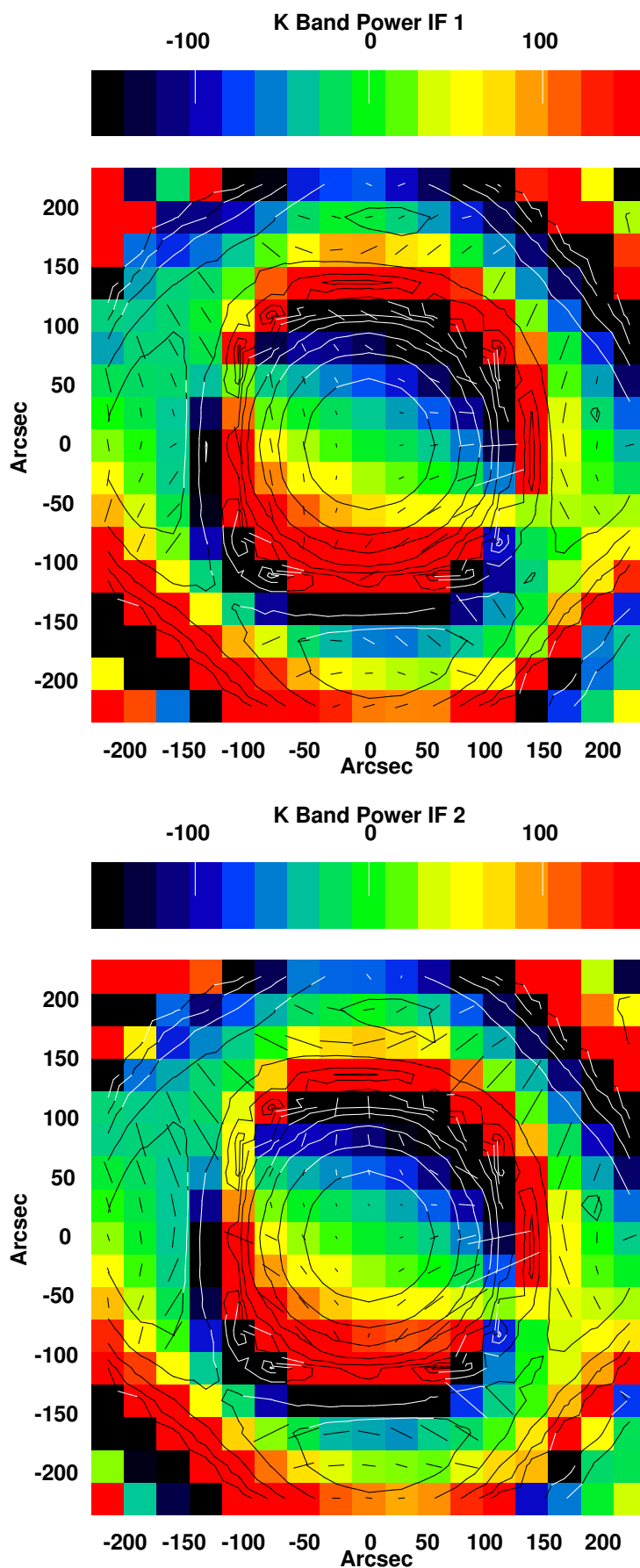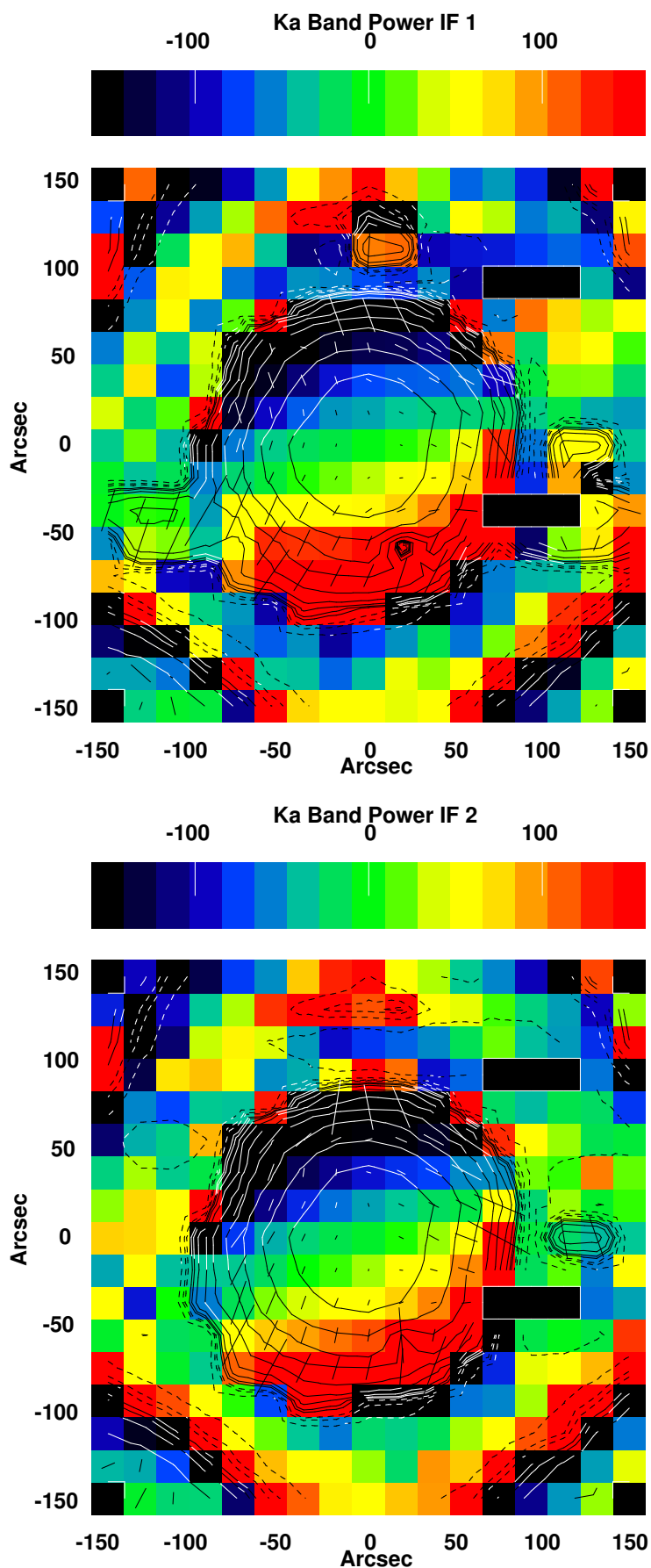
Fig. 11. Ka band power beam images in azimuth and elevation; IF 1 (33.485 GHz) upper, IF 2 (33.435 GHz) lower. Normalized total intensity is shown as contours in powers of 2 from 0.001, highest is 0.512. Stokes V is shown in color with the scale bar at the top in units of 0.001. Fractional linear polarization is represented by vectors, one pixel = 0.05.
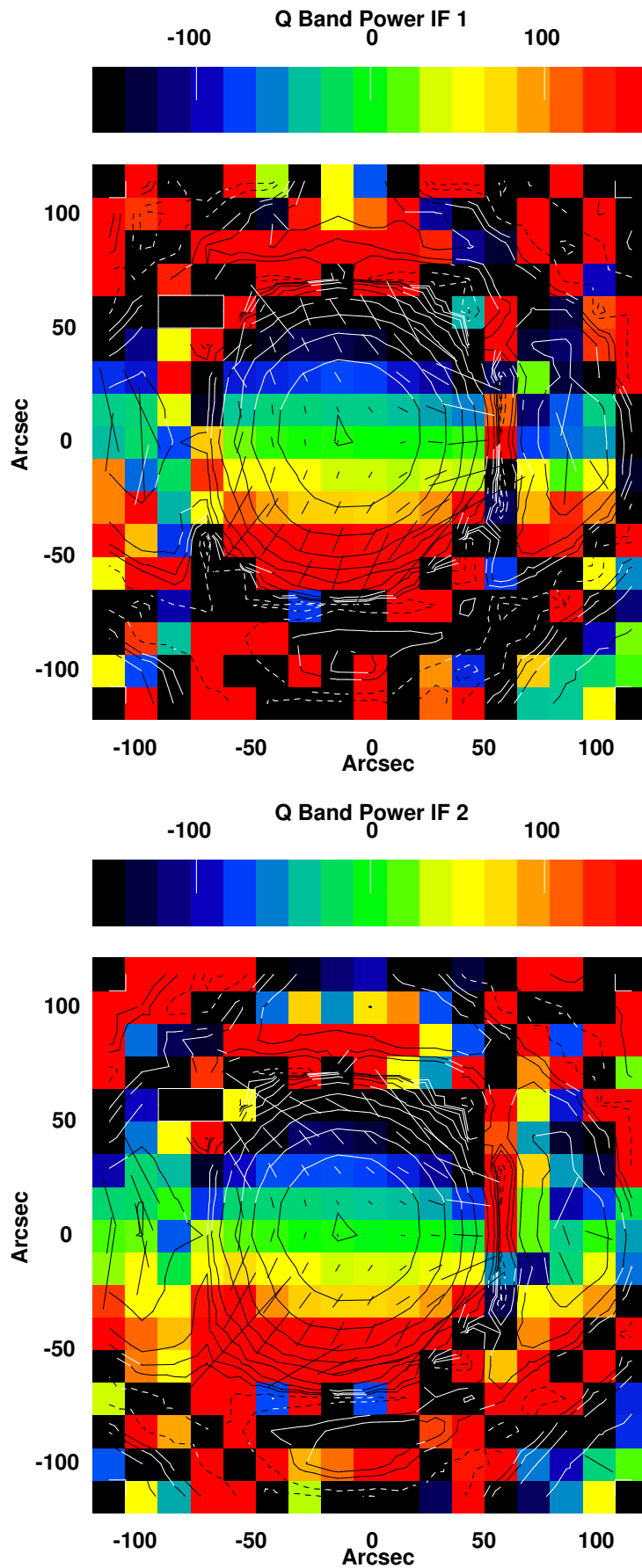
Fig. 12.   Q band power beam images in azimuth and elevation; IF 1 (43.315 GHz) upper, IF 2 (43.365 GHz) lower. Normalized total intensity is shown as contours in powers of 2 from 0.001, highest is 0.512. Stokes V is shown in color with the scale bar at the top in units of 0.001. Fractional linear polarization is represented by vectors, one pixel = 0.05.
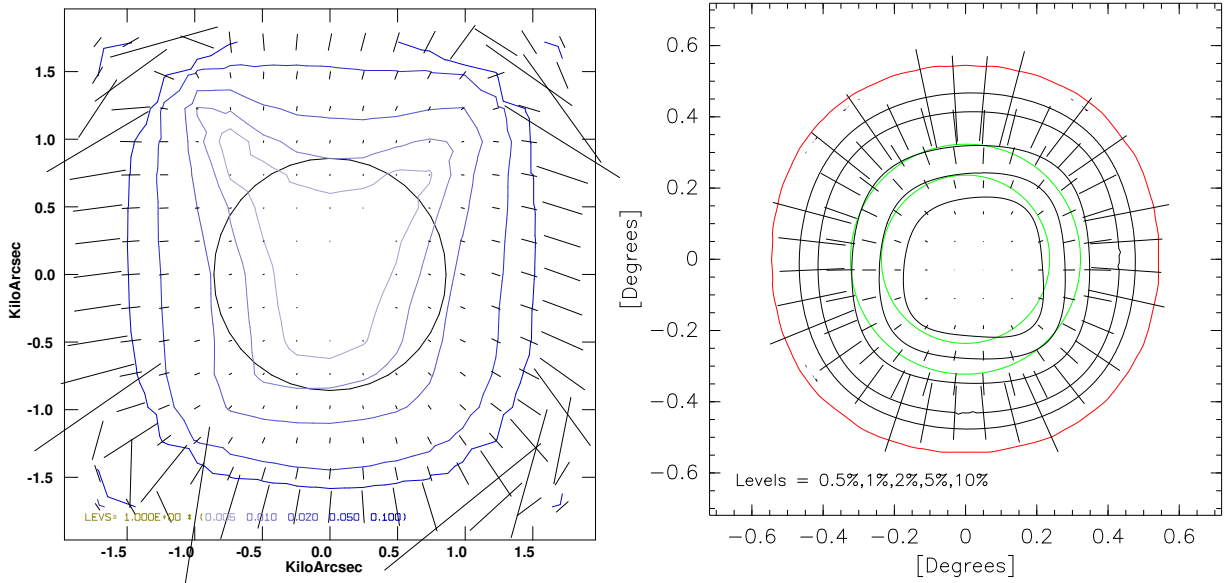
Fig. 13. The left plot shows the measured EVLA L band polarization beam at 1.465 GHz. The colored contours show the fractional linear polarization and are at 0.5, 1, 2, 5 and 10%; vectors give the orientation and magnitude of the linear polarization. The black circle shows the approximate location of the half power point of the total intensity beam.
The right plot is Figure 3 from [8] showing a model VLA beam at 1.53 GHz. The black contours show the fractional linear polarization and are at 0.5, 1, 2, 5 and 10%; vectors give the orientation and magnitude of the linear polarization. The green contours are at the 0.5 and 0.25 power points of the total intensity beam and the red contour is at the first null.

sources well removed from the center of the beam will be time variable giving rise to nonconvolutional artifacts.

This variable gain can be corrected when the sky model is used to calculate the instrumental response by the use of a correctional beam gain G'_{Ii} for model component i

$$G'_{Ii} = \frac{PB_i}{G_{Ii}}$$

where PB_i is an azimuthially symmetric beam model gain in the direction of the sky model component. For a uniformly illuminated dish, this can be approximated using a Jinc (J_1 Bessel fn(x)/x) function. Applying G'_{Ii} to the calculated Stokes I will correct the response for azimuthial asymmetries. The value of G'_{Ii} can be evaluated for each sky model component as a function of time from a beam image by computing the instaneous location in the beam and interpolating (or otherwise evaluating) the antenna beam properties. The Stokes I response of the interferometer to n point sky model components is then

$$I = \sum_{i=1}^{n} G'_{Ii} S_i \; e^{j2\pi(ux_i + vy_i + wz_i)},$$

where S_i is the flux density of sky model component i; u, v and w are the baseline spatial frequency coordinates; x_i, y_i and z_i are the component position offsets appropriate for the imaging geometry and $j = \sqrt{-1}$. Making this correction in the model subtraction portion of a CLEAN deconvolution should reduce or eliminate the artifacts due to the beam asymmetries by allowing CLEAN to converge to the correct sky model.

The off–axis feeds of antennas such as those used for the EVLA and ALMA will introduce a polarization specific "beam squint" so for the EVLA, the response needs to be computed

separately for the parallel systems of feeds as is described below. Some care is needed near the nulls of the antenna pattern.

B. Instrumental Polarization Correction

At any given instant, the off-axis instrumental polarization will be given by a function like those shown in Figures 1 – 12. The polarization pattern is fixed to the antenna, so for antennas with alt-az mounts, this pattern rotates on the sky with parallactic angle. This rotation with parallactic angle will tend to dilute this spurious polarized response, but as can be seen from Figures 1 – 12, the instrumental polarization does not change rapidly with rotation of the beam. For high accuracy polarimetry, it will be necessary to correct derived images for this instrumental polarization

Given a Stokes I sky model and images of the antenna polarized response, it is possible to estimate the interferometer response due to instrumental polarization and subtract it from the visibility data. The basic operation is fairly straightforward; to remove the response in Stokes I and corresponding off–axis instrumental polarization for an interferometer measuring circular polarizations (RR, LL, RL and LR combinations of Right– and Left–hand circular polarizations) do the following:

1) Rotate the offset of the sky model element in RA and Dec from the pointing position by the parallactic angle to get the offset in azimuth and elevation; scaling as appropriate for differences in frequency.
2) Interpolate the Stokes I, Q, U and V beam images in the appropriate frequency dependent beam images for each component of the sky model. For component i, this gives Stokes gains: G_{Ii}, G_{Qi}, G_{Ui} and G_{Vi}

3) Compute gains for RR and LL:

$$G_{RRi} = \frac{PB_i}{G_{Ii}} + G_{Vi},$$
$$G_{LLi} = \frac{PB_i}{G_{Ii}} - G_{Vi},$$

where PB_i is the azimuthially symmetric beam model gain.

4) The interferometer response for the RR and LL correlations to n components is then:

$$RR = \sum_{i=1}^{n} G_{RRi} S_i \ e^{j2\pi(ux_i + vy_i + wz_i)},$$
$$LL = \sum_{i=1}^{n} G_{LLi} S_i \ e^{j2\pi(ux_i + vy_i + wz_i)}.$$

Subtracting these values from the data should remove both the Stokes I and Stokes V response.

5) The spurious interferometer response in Q and U is similarly:

$$Q = \sum_{i=1}^{n} G_{Qi} S_i \ e^{j2\pi(ux_i + vy_i + wz_i)},$$
$$U = \sum_{i=1}^{n} G_{Ui} S_i \ e^{j2\pi(ux_i + vy_i + wz_i)}.$$

These are then counter–rotated to correct for the parallactic angle rotation in the calibration:

$$Q' + jU' = (Q + jU) \ * \ exp(-2j\chi)$$

6) The response in RL and LR correlations is

$$
\begin{aligned}
RL &= Q' + jU', \\
LR &= Q' - jU'.
\end{aligned}
$$

Subtracting these values from RL and LR will remove the Stokes Q and U responses.

7) The interpolated gains can be either real or complex.

VI. OBIT IMPLEMENTATION

The off–axis calibration scheme has been implemented in the Obit package. The ObitImageInterp class is used to interpolate beam values from image cubes of the I, Q, U and V image responses using a Lagrangian interpolator. The corrections are applied to visibility data using the c ObitSkyModelVMBeam class which can be used for any operation in Obit requiring the calculation of an interferometric response to a CLEAN sky model. In order to speed the computations, the model calculation uses multi–threaded operation when available[9] and uses a fast vector sincos routine[10]. User accessible interfaces to this class are through the python class SkyModelVMBeam and task UVPolCor which applies the corrections while subtracting a Stokes I CLEAN model from a visibility dataset; corrections can also be applied during imaging in Obit task BeamCor.

VII. CORRECTION TESTS

In order to test the usability of the above technique for correcting off–axis instrumental effects, pointed observations of the bright sources used for the beam measurements were made at the half power of the beam at a series of orientations every $45°$ from south (on the sky) through west to north. These observations were obtained at the same time as the beam images and used the same frequency and correlator settings as well as a common calibration. The "low" resolution beam images were used for these tests and were applied in Obit task UVPolCor followed by imaging in Obit task Imager.

These observations for L, C and X band are summarized in Table I. The first four columns of this table give the I, Q, U and V flux densities at the position of the source with no corrections. The column "Squint V", is the value of the Stokes V image as generated by Obit task Squint (see section VII-A) which corrects for beam squint. The columns labeled "RRes S" are the Stokes "S" residual corrected using only the real part of the beam image. The columns labeled "CRes S" are the Stokes "S" residual corrected using the complex beam image. An example is shown in more detail below.

A comparison of the Stokes I, Q, U and V images at C band with and without corrections using the "real" beam patterns for one of these test observations is shown in Figures 14 – 17. The uncorrected Stokes I image has a peak of 5.6 Jy/beam, Stokes Q 77 mJy/beam, Stokes U -122 mJy/beam and Stokes V 300 mJy/beam. Only the Stokes U residual image contains a response to the source greater than the noise at -23 mJy/beam.

A full complex correction was also applied to test if the residuals were due to the phase response of the antennas. The residual images are shown in Figure 18. There is no signifigant difference between the real and complex corrections. Table I shows this to be more generally true.

A. Comparison with Obit task Squint

An alternate method to remove the off-axis instrumental circular polarization from VLA data is using Obit task Squint [7] in which an assumed beam shape and the known geometry of the feeds is used to calculate the offset of the positions of the RCP and LCP beams. A comparison of the corrected image shown in Figure 17 and one obtained using Squint is given in Figure 19. The RMS residual in the two images is 8.6 mJy/beam for Squint and 8.3 mJy/beam for the image derived from the measured beam polarization. Both images show residuals above the noise level, the ones from Squint are somewhat stronger. Other comparisons are given in Table I.

B. Holography Resolution

In order to evaluate the effects of the resolution of the holographic beam maps on the accuracy of the corrections obtained from these beam images, a set of tests were performed comparing using the high and lower resolution beam images. The tests used Obit task BeamCor to apply the corrections while imaging. The resultant polarized residuals from the comparison are given in Table II in a comparison
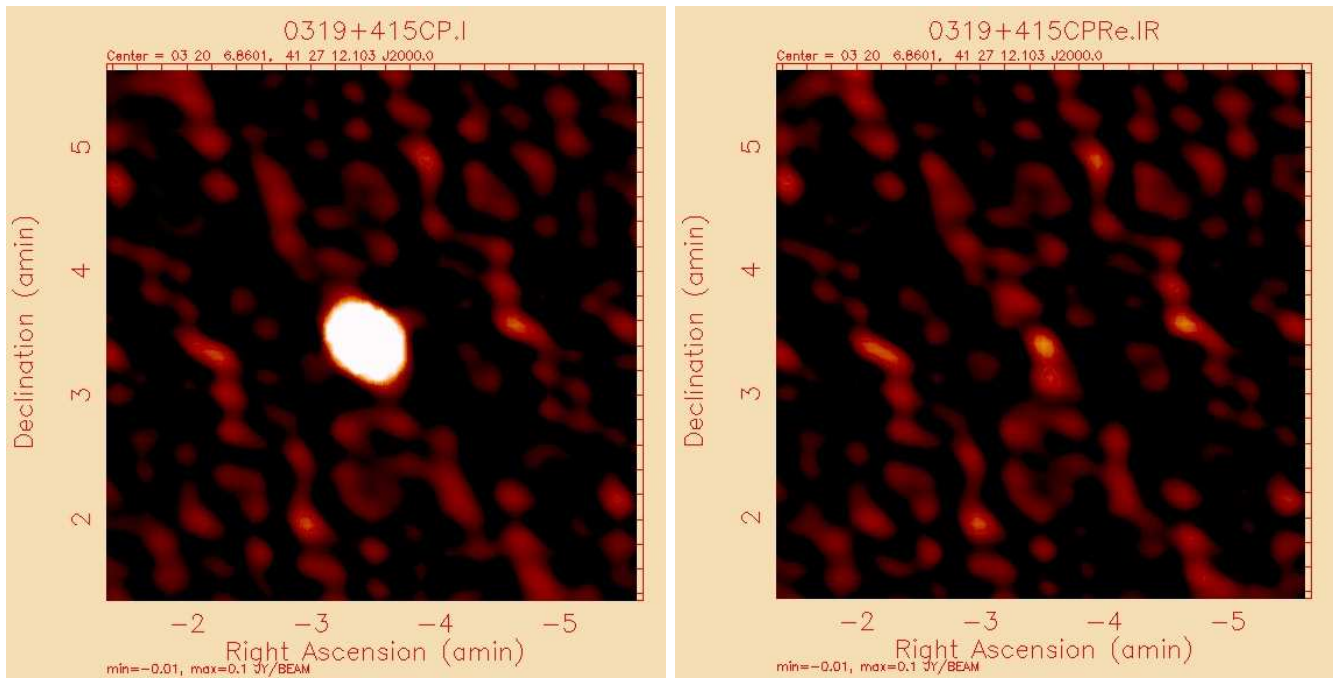
Fig. 14.   C band pointing P Stokes I test real correction. Images with linear stretch from -0.01 to 0.1 Jy, uncorrected peak = 5.6 Jy. **Left:** uncorrected, **Right:** corrected.

Fig. 15.   C band pointing P Stokes Q test real ccorrection. Images with linear stretch from -0.05 to 0.05 Jy, uncorrected peak = 77 mJy. **Left:** uncorrected, **Right:** corrected.

Fig. 16.   C band pointing P Stokes U test real ccorrection. Images with linear stretch from -0.05 to 0.05 Jy, uncorrected peak = -122 mJy. **Left:** uncorrected, **Right:** corrected.

Fig. 17.   C band pointing P Stokes V test real ccorrection. Images with linear stretch from -0.1 to 0.1 Jy, uncorrected peak = 300 mJy. **Left:** uncorrected, **Right:** corrected.
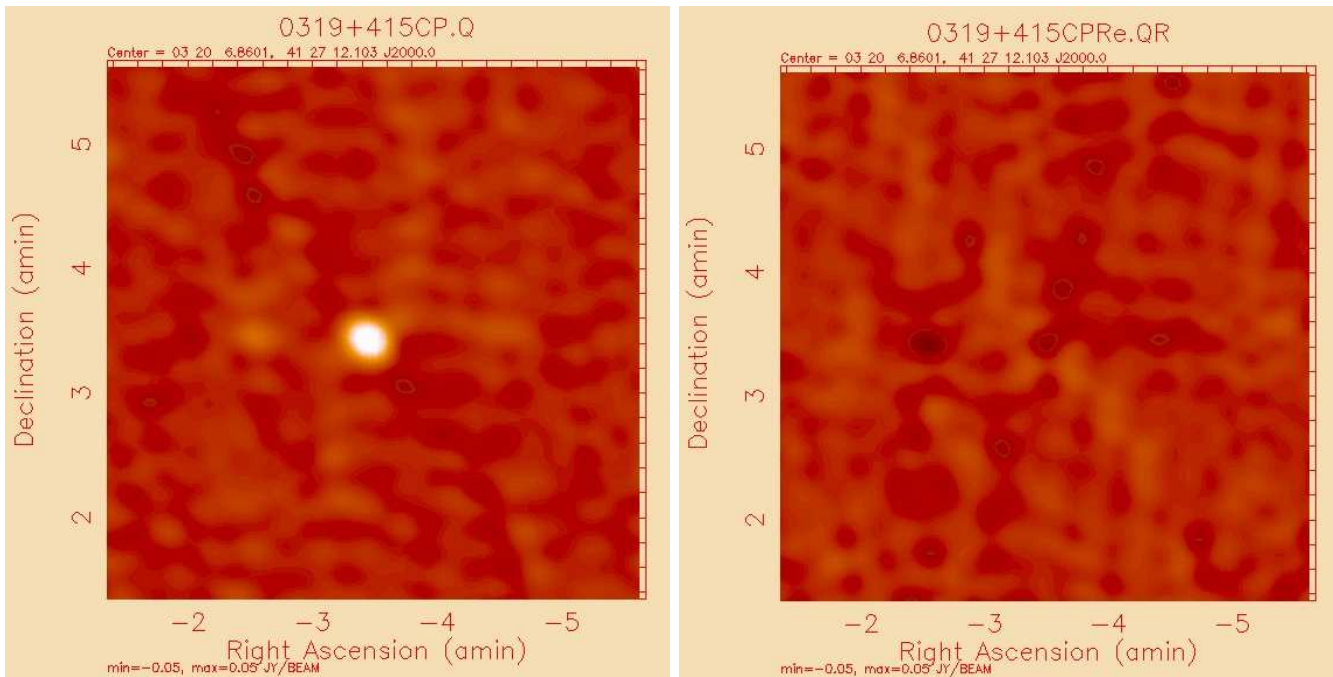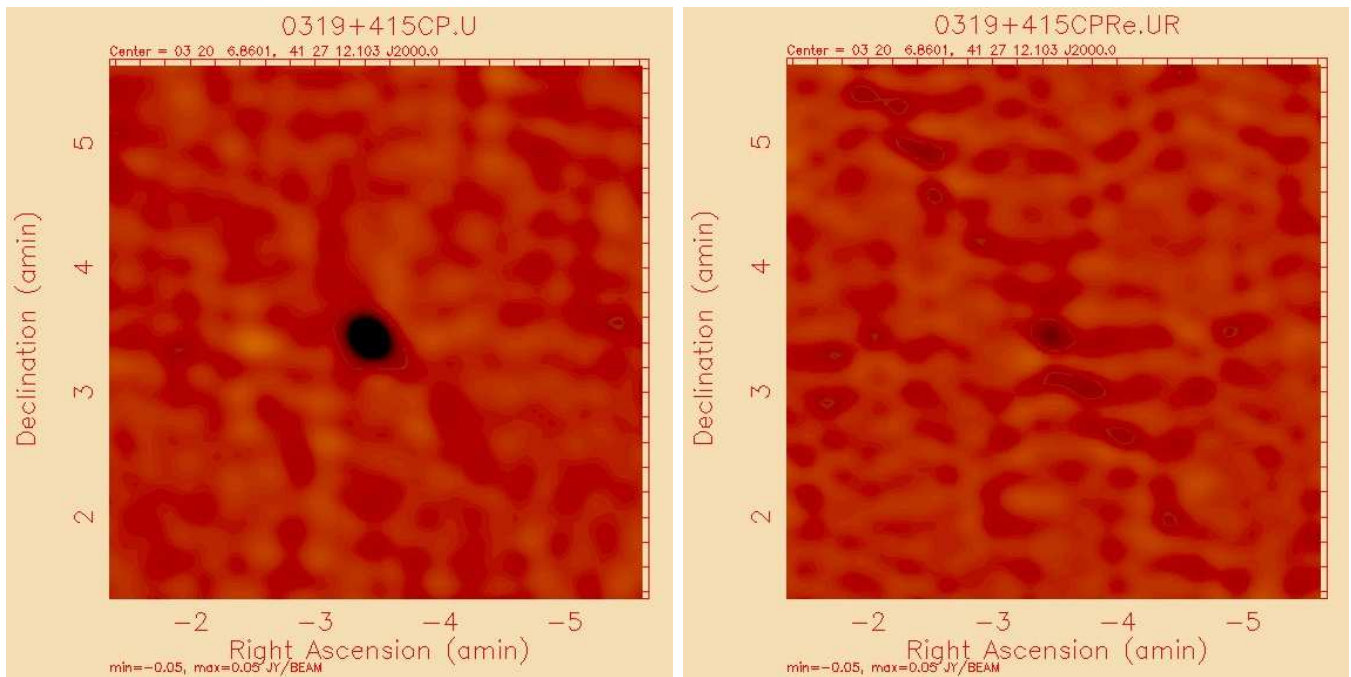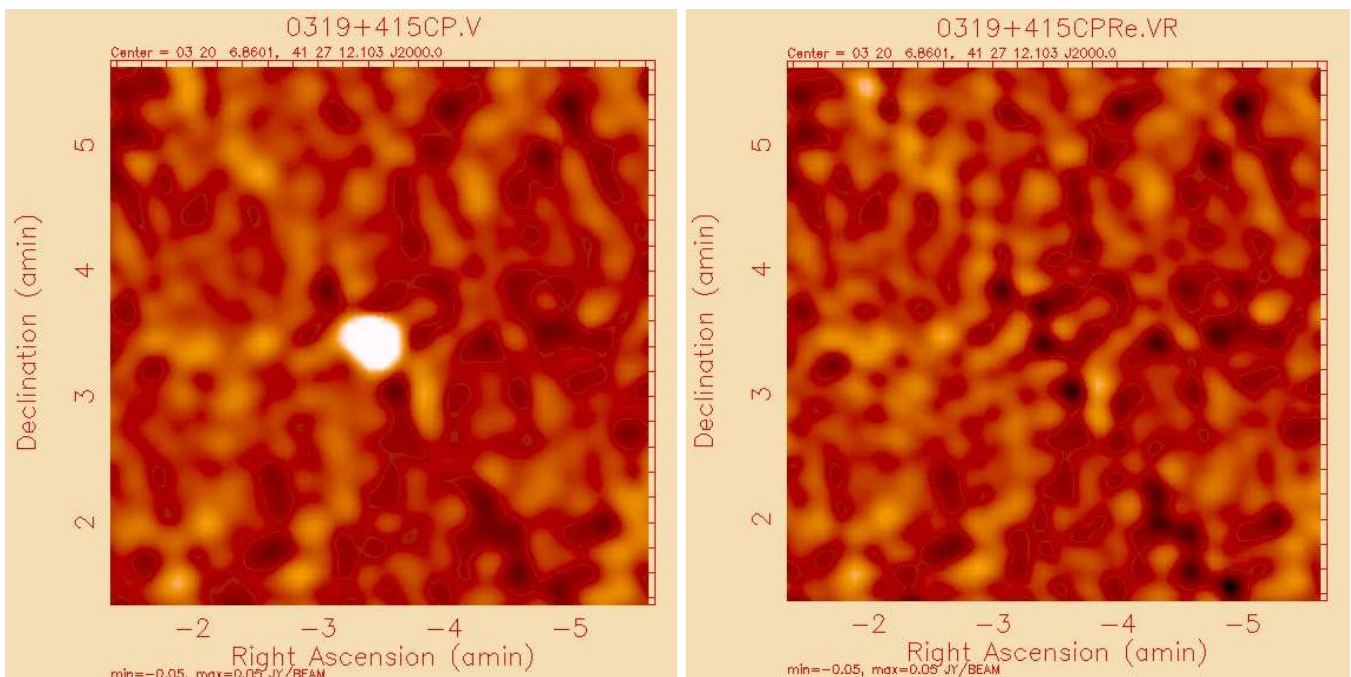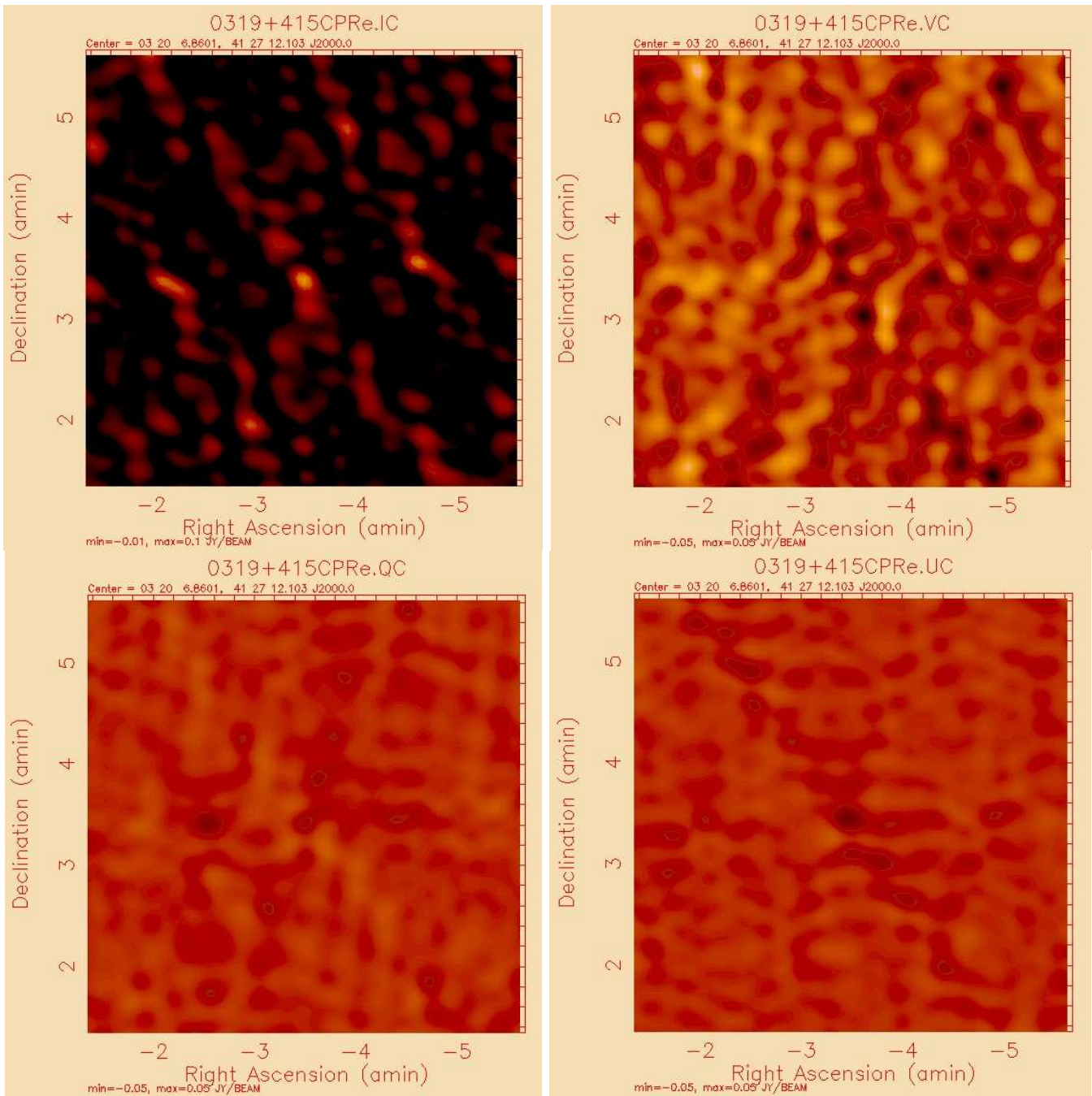
Fig. 18.   C band pointing P complex correction test. Top left is Stokes I, top right, Stokes V, bottom left is Stokes Q and bottom right is Stokes U residuals.

similar to that presented in Table I. The results of this test show that the high resolution beam image gave slightly higher residuals. However, the high resolution image was made at a different frequency while the low resolution beam image used the same calibration as the test data. Note: the total intensities derived are more consistent when the corrections are applied in imaging (Table II) than when they are not (Table I), demonstrating the correction of azimuthal asymmetries

VIII. DISTRIBUTION OF BEAM IMAGES

The beam images are available on the NRAO-CV ftp server at   ftp://ftp.cv.nrao.edu/NRAO-staff/bcotton/Obit/BeamImages

as gzipped FITS images. File names begin with the Stokes value (I,Q,U,V) followed by "Ph" for phase images, followed by "BeamMap". Then the band code, e.g. "Xband", for the "real" beam images and a single letter code, e.g. "X", for the phase images.

IX. DISCUSSION

Some general comments may be made about the beam images in all frequency bands. In Stokes I, the central part of the beam is relatively symmetric but this symmetry is lost past the null and is replaced by a four-fold symmetry. This pattern is presumed the result of the sub-reflector support legs.

TABLE I
POINTED OBSERVATION TESTS

| source	band	pointing	I	Q	U	V	Squint V	RRes Q	RRes U	RRes V	CRes Q	CRes U	CRes V
			Jy	mJy	mJy	mJy	mJy	mJy	mJy	mJy	mJy	mJy	mJy
0542+498	L	L	10.400	132.0	73.2	-765.0	114.1	38.1	0.4	126.8	37.5	-0.4	125.1
0542+498	L	M	9.863	133.3	13.3	-685.0	62.0	46.0	-3.0	27.3	45.4	-2.7	22.0
0542+498	L	N	9.722	-36.8	-54.2	-111.8	64.7	-6.4	-1.7	-53.6	-13.1	3.0	-53.7
0542+498	L	O	9.897	-59.1	63.0	371.2	-116.6	-21.6	-0.5	-188.0	-21.5	-0.6	-187.6
0542+498	L	P	9.513	74.9	117.7	767.4	-108.3	-23.6	14.6	-3.0	-22.4	13.8	-5.6
0319+415	C	M	5.717	26.7	-19.6	61.8	-60.4	-27.5	36.4	-43.3	-27.2	36.3	-32.0
0319+415	C	N	5.873	-33.1	39.0	451.2	-59.7	-40.7	-0.6	-23.8	-38.3	-1.0	-23.2
0319+415	C	O	5.792	-22.1	-19.5	546.3	-59.7	-19.6	-28.1	-21.7	-16.1	-26.7	-21.5
0319+415	C	P	5.888	76.6	-122.4	299.5	-41.5	-9.1	-23.3	-26.4	-7.6	-23.6	-25.5
0319+415	C	Q	5.565	77.8	-55.5	-116.4	28.9	-6.3	-12.0	13.5	-6.5	-11.3	10.0
0319+415	X	L	7.263	47.5	21.7	512.7	-51.6	3.5	-4.4	42.8	3.6	-3.0	43.2
0319+415	X	M	7.628	-10.0	77.7	758.7	-32.0	-0.7	14.4	53.6	-0.8	14.4	55.0
0319+415	X	N	7.911	-49.8	5.6	494.4	-41.4	-23.5	3.8	-0.7	-23.5	3.7	-0.3
0319+415	X	O	8.174	14.1	-98.1	-41.6	49.8	-19.8	-24.8	11.8	-19.8	-24.8	11.6
0319+415	X	P	6.574	60.6	-50.7	-517.6	89.4	0.3	-12.5	0.9	0.2	-12.5	0.9
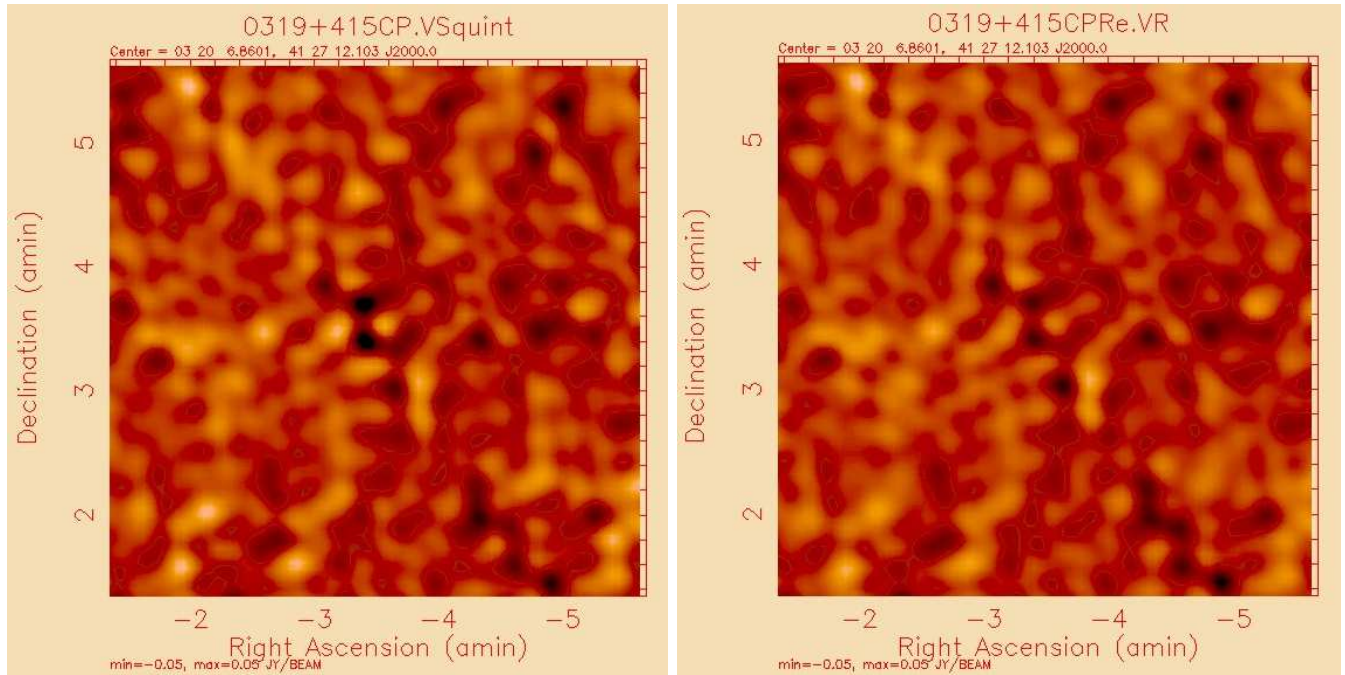
Fig. 19.   Comparison of Stokes V correction derived using a measured beam model and one computed using ObitTask Squint Images with linear stretch from -0.1 to 0.1 Jy, uncorrected peak = 300 mJy. **Left:** Image from Obit task Squint, RMS = 8.6 mJy/Beam. **Right:** From Figure 17, RMS = 8.3 mJy/Beam.

TABLE II
HOLOGRAPHY RESOLUTION TEST

source	band	pointing	I	High Res Q	High Res U	High Res V	Low Res Q	Low Res U	Low Res V
			Jy	mJy	mJy	mJy		mJy	mJy
0542+498	L	L	10.042	-5.6	29.7	18.4	-17.1	26.5	36.8
0542+498	L	M	10.098	35.3	8.4	-3.9	27.0	-13.0	17.3
0542+498	L	N	10.227	8.8	22.1	-29.3	10.1	-8.5	-91.2
0542+498	L	O	10.122	35.0	-7.9	-253.2	25.0	-6.6	-200.4
0542+498	L	P	10.002	29.4	-38.3	-56.5	19.5	-19.8	-47.9

The average antenna power patterns shown in Figures 14 – 17 show the expected increase of residual instrumental linear polarization after on–axis calibration from zero on–axis to very substantial ($\sim$10%) in the first side-lobe. In the more strongly polarized portions of the beams, the images in the two IFs (usually adjacent 50 MHz bands) are very similar suggesting that these patterns may not need to be measured with fine frequency resolution. The general pattern of linear polarization is seen among all beam images with the polarization of the side-lobes following the four–fold symmetry of the Stokes I, presumably also due to the sub-reflector support legs.

The off-axis instrumental circular polarization is quite strong due to the beam squint of the off–axis feeds and exceeds 10% even in usable portions of the main beam. The orientation of the instrumental circular polarization pattern is determined by the orientation of the corresponding feed on the feed circle.

The measured linear polarization beams are compared with the results of modeling by Walter Brisken using GRASP8[8] in Figure 13 although this is comparing the VLA with EVLA feed configurations and is only for L band. The polarization vectors in Figure 1 and 13 have generally the same orientation as in Brisken's Figure 3 with differences up to few 10's of degrees. Brisken's Figure 3 has the linear polarization varying between 0.5 and 1% at the half power circle. Values from Figure 1 and Table I give similar but somewhat larger values. The model linear polarization has a center offset from the center of the total intensity beam whereas the measured beams do not.

A technique is presented which largely corrects the off–axis instrumental polarization; for Stokes V, the method generally does a better job in removing instrumental circular polarization than that used in Obit task Squint which is based on an analytical model. In one test, correction of the linear polarization of a very bright source observed at the 50% power point of the beam reduced the polarized response from 2.2% of Stokes I to 0.4% ,leaving a visible residual of the source. Other comparable results are given in Table I. Making corrections based on the full complex beam images gives comparable results to using only the "real" beam images. The resolution of the beam images appear not to be the limitation of the accuracy of the correction.

The correction technique shows promise, corrections are generally good to a few parts per thousand of the Stokes I response at the beam half power. However, the limitations are not currently understood.

References

[1] W. D. Cotton, "Obit: A Development Environment for Astronomical Algorithms," *PASP*, vol. 120, pp. 439–448, 2008.

[2] E. B. Fomalont and R. A. Perley, "Calibration and editing," in *Synthesis Imaging in Radio Astronomy*, ser. ASP Conference Series, R. A. Perley, F. R. Schwab, and A. H. Bridle, Eds., no. 6. Astronomical Society of the Pacific, 1989, pp. 83–114.

[3] J. J. Condon, W. D. Cotton, E. W. Greisen, Q. F. Yin, R. A. Perley, G. B. Taylor, and J. J. Broderick, "The NRAO VLA Sky Survey," *Astron. J.*, vol. 115, pp. 1693–1716, May 1998.

[4] W. D. Cotton, "Widefield Polarization Correction of VLA Snapshot Images at 1.4 GHz," *AIPS Memo Series.*, vol. 86, pp. 1–9, 1994.

[5] P. J. Napier and J. J. Gustincic, ""polarization properties of a cassegrain antenna with off-axis feeds and on-axis beam.","" in *"Digest of the IEEE International Symposium"*, ser. "Stanford: IEEE Antennas and Propagation Society", 1977, pp. 452–454.

[6] P. J. Napier, "Polarization Properties of an Open Cassegrain Antenna," *MMA Memo*, vol. 115, pp. 1–17, 1994.

[7] J. M. Uson and W. D. Cotton, "Beam squint and Stokes V with off-axis feeds," *A&A*, vol. 486, pp. 647–654, 2008.

[8] W. Brisken, "Using GRASP8 to Study the VLA Beam," *EVLA Memo Series.*, vol. 58, pp. 1+, 2003.

[9] W. D. Cotton, "Note on the Efficacy of Multi-threading in Obit," *Obit Developement Memo Series*, vol. 1, pp. 1–8, 2008.

[10] ——, "A Fast Sine/Cosine Routine," *Obit Developement Memo Series*, vol. 14, pp. 1–9, 2009.